IS-PORTO 2023 PROCEEDINGS

Proceedings of the 8th International Symposium on DEFORMATION CHARACTERISTICS OF GEOMATERIALS Porto, 3rd - 6th September 2023

Sand and silt treatment with novel binders

Giovanni Spagnoli[1], *Alessandro* Fraccica[2], *Marcos* Arroyo[3,4#] and *Enrique* Romero[3,4]

[1]*DMT GmbH & Co. KG, Am TÜV 1 45307 Essen, Germany*
[2]*Italian Institute for Environmental Protection and Research, ISPRA, Via Brancati 48 00144 Rome, Italy*
[3]*Universitat Politecnica de Catalunya, Department of Civil and Environmental Engineering, C. Jordi Girona 1-3 08034 Barcelona, Spain*
[4]*Geomechanics Group, International Centre for Numerical Methods in Engineering, C. Gran Capitá S/N 08034 Barcelona, Spain*
[#]*Corresponding author: marcos.arroyo@upc.edu*

ABSTRACT

An attractive approach to reduce the carbon footprint for ground improvement application is to replace Portland cement-based binders by non-cementitious binders for instance by geopolymers based on metakaolin in deep soil mixing applications or by colloidal silica and acrylates in permeation based applications. Safe design requires a good understanding of the mechanical and hydraulic properties of the improved ground but little is known about how soil is improved by these products. Besides, for permeation grouting applicability criteria are frequently set in terms of the host soil water permeability. However, for novel binders the threshold value is not known and published empirical basis for available criteria is relatively scarce. This paper summarizes results from a laboratory characterization campaign of soils of variable permeability improved with different novel binders, focusing on the effect on strength, stiffness and permeability. Observations relative to the effect of curing conditions are also provided, as well as the insight gained by examining the injection process outcomes with computed tomography. Results show how these novel products have the potential to significantly improve the mechanical properties and reduce permeability in a large range of soils.

Keywords: Sand; silt; permeation grouting; deep-soil mixing; hydro-mechanical properties.

1. Introduction

The methods of ground improvement are aimed at modifying the engineering properties of natural soils such as resistance, deformability and permeability. Ground improvement techniques can be divided into three broad groups: 1) those based on processes that modify soil properties by external action without any inclusion or additive (e.g. preloading or dynamic compaction) 2) those requiring the insertion of distinctive elements in the soil, typically metallic or plastic materials, such as those required in geosynthetic or steel earth reinforcement 3) those who modify the nature of the ground by adding in some new component that is mixed or injected in the soil (Colombo and Colleselli 1996).

In this latter category we find a number of technologies differing in the amount of energy that they apply to affect the mixture of soil and additive and, consequently, on the disruption that they impose on the original soil structure (e.g. Moseley and Kirsch 2004; Croce et al. 2014; Han, 2015). The less disruptive is permeation grouting and the most disruptive is jet grouting, with technologies like hydrofracturing, compaction grouting, and deep soil mixing somewhere in the middle. The technology selected will also depend on the nature of the soil and of the additives. Products such as lime, cement, mortar, calcium chloride, sodium, ash, but also chemical binders such as resins, polymers, and sodium silicate have been employed (Colombo and Colleselli 1996; Moseley and Kirsch 2004; Nicholson 2015). The variety is more apparent than real, as cement based treatment are by far the more usual.

The production of cement contributes 8% of the world's carbon dioxide (CO_2) emissions, therefore it is becoming more urgent to reduce the carbon footprint of concretes (IEA 2018). To significantly reduce emissions over the long run, low-carbon binders in which Ordinary Portland Cement (OPC) has been completely substituted are essential (Lehne and Preston 2018). This is consistent with the idea that material use dominates the environmental impact of geotechnical systems across their entire life cycle (Kendall et al. 2017). Life-cycle carbon emissions have been suggested as a way to assess the global environmental impact of certain projects, namely ground improvement (Shillaber et al. 2016). Therefore, it seems likely that the path to sustainable ground improvement would increasingly involve low-carbon, alternative binders (Mohammed et al. 2021). This is one of the main drivers behind the push for new binders in ground improvement applications (e.g. Han 2015; Fraccica et al. 2022a; Salvatore et al. 2022; Spagnoli 2021; Spagnoli et al. 2022a).

The paper presents some data regarding the application of metakaolin, colloidal silica and an acrylic resin for ground improvement by injection and/or mixing with soils such as a quartz sand, a carbonate silt and a low plasticity silt. The data was obtained as a result of an extensive research program performed over the last four years, see Spagnoli et al. (2021; 2022b) and Fraccica et al. (2022a;b;c; 2023) which is here summarized.

2. Materials and methods

The base soil selected to prepare the treated samples is Holcim quartz sand (0.2-0.6mm), hereafter indicated as "sand" or "S", with a SiO_2 content of 93%. The physical properties of this sand are presented in Spagnoli et al. (2022b) and Fraccica et al. (2022a;b). To reduce the permeability two types of silt were mixed with the sand: a carbonate silt, abbreviated as "O" (see Spagnoli et al. 2022b) and a silt (hereafter indicated as "silt" and "T") obtained by sieving a low-plasticity silty sand described by Fraccica (2019) and Fraccica et al. (2022a). The pre-treatment permeability of the base soils and soil mixtures was evaluated by rigid wall permeameter tests and is presented in Table 1, jointly with the pre-treatment void ratio at which tests were conducted.

Table 1. Base soils and mixtures with their pre-treatment permeability and initial (pre-treatment) and average final (post-treatment) void ratio

Soil Abbreviation	Description	*k* *(m/s)*	Initial void ratio (-)	Average final void ratio (-)
S	Fine sand	$7.7\text{x}10^{-4}$ [a]	0.825 [a]	0.538 [a]
S+10%O	Fine sand + 10% of carbonate silt (*w/w*)	$2.9\text{x}10^{-4}$ [a]	0.584 [a]	0.471 [a]
70%S+ 30%T	70% of fine sand + 30% of low-plasticity silt	$1.2\text{x}10^{-4}$ [b]	0.688 [b]	n.a.
45%S+ 55%T	45% of fine sand + 55% of low-plasticity silt	$3.9\text{x}10^{-5}$ [b]	0.687 [b]	n.a.
30%S+ 70%T	30% of fine sand + 70% of low-plasticity silt	$5.6\text{x}10^{-6}$ [b]	0.687 [b]	n.a.
T	low-plasticity silt	$2.0\text{x}10^{-7}$ [b]	0.689 [b]	n.a.

[a]Spagnoli et al. (2022b) [b]Fraccica et al. (2022a)

Three types of binders were used to improve the soil:

1. a metakaolin, here abbreviated as MK. MK is dehydroxylated aluminium silicate activated with liquid potassium silicate ($w(SiO_2)/w(K_2O)$ = 1) and water, with a liquid/metakaolin mass proportion equal to 2;
2. a colloidal silica, here abbreviated as CS, an aqueous dispersion (density 1.30 Mg/m^3) with silica concentration of either 15% or 40% and activated by a solution of NaCl (10% *w/w*) and;
3. an acrylic resin, here abbreviated as RE, mixed with an accelerator (Part A) in a volumetric ratio of 1, with water and hardener (0.35% *w/w*) (Part B).

The characteristics of these binders are detailed in Spagnoli et al. 2022b and Fraccica et al. (2022a;b).

As different types of binders were employed, the sample preparation was different. MK slurry is highly viscous and cannot be used for injection; the only realistic path for application in ground improvement is through mixing. Therefore, after being activated with liquid potassium silicate, resulting binder slurry was hand-mixed with clean sand or sand containing carbonate silt after being agitated with a mixer to achieve a lump-free dispersion (Spagnoli et al. 2022b), see Fig. 1A. The amount of binder slurry mixed with soil was chosen to fill either 100% or 40% of the soils' pre-determined as-poured porosity. Once obtained the soil-MK mixture, this was poured in moulds to cure.

Colloidal silica and acrylic resin, on the other hand, are suitable for injection treatment. After being activated, they were pumped into a previously compacted soil, contained in a mold. Injection pressures were kept below 200kPa, to achieve permeation i.e. injection in which the structure of the soils is not modified. Injections always lasted 45 minutes to remain below the binders' open time and to avoid clogging the laboratory equipment's lines. Detailed information on the lab permeation procedure is given in Fraccica et al.; 2022a;b and in Spagnoli et al. 2022b. Fig. 1B shows the injection layout for colloidal silica samples.

Initial void ratio values for the host soils were kept in the order of 0.6 to 0.8 (see Table 1). These void ratios were assumed to be constant across the soil height (X-ray images will be further presented to check the assumption and the homogeneity of binder's permeation). In samples with final void ratio measurements, the effects of void ratio and specific surface of the grouted soil were correlated to the final permeability and unconfined strength (Spagnoli et al. 2022b).

The effects of curing were explored, particularly for the metakaolin based mixtures, as in deep soil mix the treated soil and its surroundings need not be saturated or underwater. Indeed, for some applications, such as retaining walls, the soilcrete might be quickly exposed to the atmosphere. Spagnoli et al. (2022b) describe two different curing environment: "dry curing" (D) referred to specimens that are cured in a chamber at 20°C and 50% relative humidity (RH), whereas specimens cured at 100% relative humidity and at 20°C are referred to as wet curing (W).

Different geotechnical tests were performed on the improved soils: unconfined compressive strength (UCS) tests, permeability tests (k-values) measured in a triaxial cell under controlled hydraulic gradient, isotropically consolidated undrained triaxial compression tests (TXCIU), cyclic triaxial loading, direct shear and long-term oedometric creep tests. Apart from those tests, mercury intrusion porosimetry (MIP), Field Emision Scanning Electron Microscopy (FESEM) and X-Ray tomography were systematically applied to observe the treated soils at the microscale. For detailed information about the laboratory preparation and methodology, it is suggested to consult Spagnoli et al. 2022b; Fraccica et al. 2022a; 2022b; 2023. Table 2 summarizes the tests that will be presented in this paper. All these results refer to samples with 28 days of curing.

Table 2. Procedures and number of tests with respect to different soil mixtures, binders, and curing conditions (D = curing at 20°C and 50% relative humidity, W = curing at 20°C and 100% relative humidity) investigated. S = sand, T = silt, CO = carbonate silt. *k* = post-treatment water permeability, *E* = Secant Young Modulus at 50% of the unconfined compressive strength *(UCS)*

Soil (*w/w*)	Binder/ Sample preparation	*k*	*UCS* and *E*	X-ray tomogr.
S	MK/ mixing CS/ injection after soil dry pouring in moulds	MKx12(D)[b] MKx5(D)[c] CSx6(D)[b]	MKx4(D)[ce] MKx4(W)[ce] CSx3(D)[e]	MKx2(D)[d]
S+10% O		MKx9(D)[b] MKx6(D)[c] CSx6(D)[b]	MKx3(D)[ce] CSx5(D)[e]	MKx1(D)[d]
70%S+ 30%T	CS-RE/ injection after soil static compaction	-	CSx4(W)[a] REx2(W)[a]	CSx2(W)[a] REx3(W)[a]
45%S+ 55%T		-	CSx4(W)[a] REx2(W)[a]	CSx2(W)[a] REx1(W)[a]
30%S+ 70%T		-	CSx5(W)[a] REx2(W)[a]	CSx2(W)[a] REx1(W)[a]
T		-	CSx2(W)[a] REx2(W)[a]	CSx2(W)[a] REx2(W)[a]

[a]UC tests, Fraccica et al. (2022a); [b]consolidated undrained static triaxial tests, Fraccica et al. (2022b) [c]consolidated undrained static triaxial tests, Spagnoli et al. (2022b) [d]X-ray equipment, Spagnoli et al. (2022b) [e]UC tests, Fraccica et al. (2022b)

3. Results and discussion

3.1. Unconfined compressive strength

Fig. 2 shows the results of UCS tests performed on the different soil mixtures. The strength of soils treated with MK, was very much higher than that of the other mixtures, reaching UCS values above 1MPa

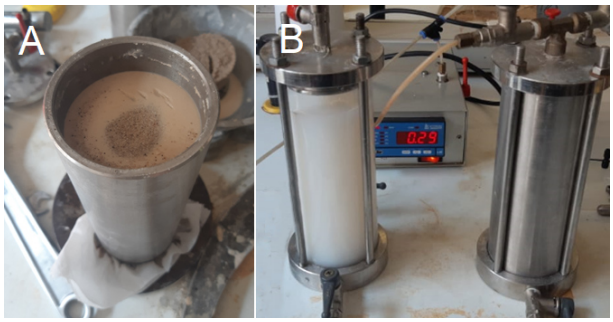

Figure 1. Preparation of the MK samples (A) and of the colloidal silica samples (B).

An interesting observation is that whereas adding more silt was generally detrimental to strength in the permeated materials, that was not the case for the MK mixtures. This was related to the curing condition for the MK which was a dry one and was clarified through microscale study.

Curing conditions have an impact on the pore size distribution. The volume of the macropores decreased as a result of wet curing. Dry curing led to a definite increase in macropore volume and a minor decrease in overall micropore volume as the lower mode distribution sharpened (Spagnoli et al., 2022b). When carbonate silt is present, both the micropore and the macropore peaks increase for the same dry curing setting. As a result, while micropores were usually prominent in MK mixed with sand, the macropore and micropore fractions are more evenly distributed in samples where MK was mixed to sand + carbonate silt.

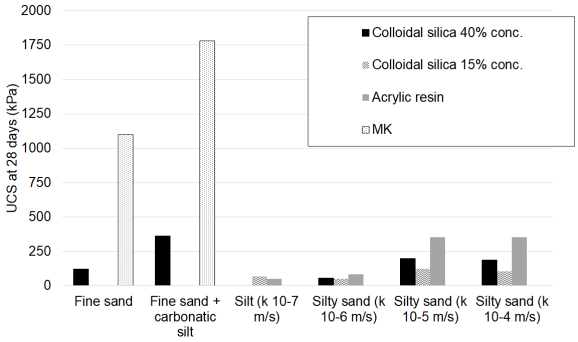

Figure 2. UCS tests at 28 days for the binders used in different soils (modified after Spagnoli et al. 2021; 2022b) and Fraccica et al. 2022a;b).

The FESEM data shed some more light on this issue. Images of sandy samples with the carbonate silt at various magnifications show that carbonate silt seems to coat the sand grains rather than fill spaces between the grains (Spagnoli et al., 2022b). The reaction of the sand + carbonate silt mixed with MK was influenced by this phenomenon. Fig. 3 shows that compared to the sample without silt (left), the sample with silt (right) displayed greater relative movements and separation between sand grains. The extremely fissured nature of the MK between sand grains is clear in the FESEM images.

As for the other mixtures in Fig. 1, in general UCS values are below 500kPa at 28 days for the injected soils. This is in good agreement with the latest results of Spagnoli and Tintelnot (2022c) where the same type of colloidal silica with 40% concentration reached values of about 533kPa at 28 days injected into the Frechen quartz sand (0.16mm).

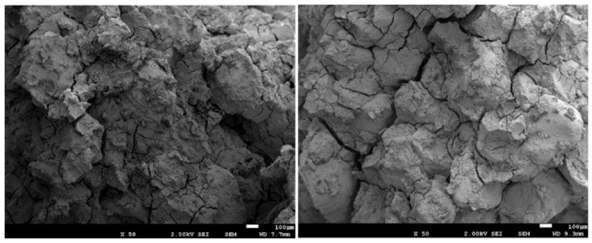

Figure 3. FESEM of sand + MK (left) and sand + carbonate silt + MK (right) cured at 50% after 28 days.

The results obtained with CS with 40% concentration, at 28 days of curing, are compared with those observed in literature for different SiO_2 concentrations and different curing conditions (see Fig. 4). The grouted sand with colloidal silica lies slightly below the trend from previous observations, while the grouted sand + carbonate silt are in good agreement with other results from the other authors.

The behavior of soil treated with CS grout is evidently quite complex based on the state of the science at this time. It is worth noticing that the strenght improvement

depends on factors such as CS solid content and curing type. Besides, in terms of strength development, it is still unclear whether fully humid storage conditions are advantageous (Axelsson 2006) or disadvantageous (Persoff et al. 1999). However, a transient groundwater table with variable RH in the soil is simulated using a RH of 50%.

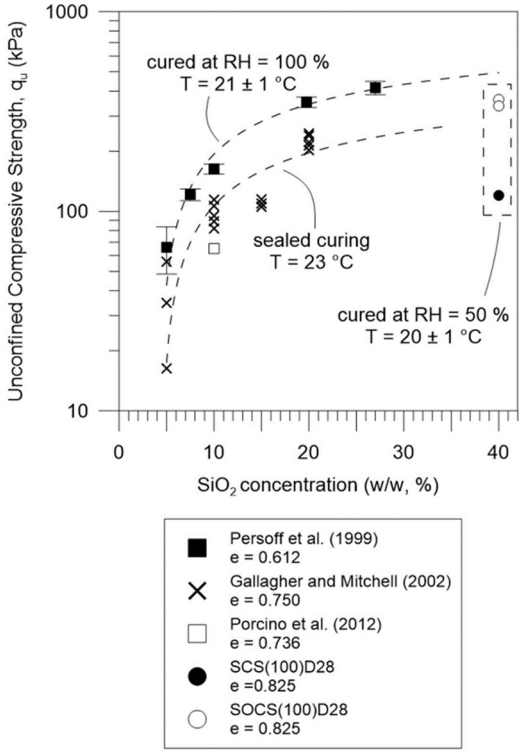

Figure 4. UCS relation with SiO_2 concentration in colloidal silica. SCS stands for sand grouted by colloidal silica. SOCS stands for sand + carbonate silt grouted by colloidal silica. For the data from the authors 100 is the percentage of voids filled and D stands for cured at 50% RH.

3.2. Stiffness

In Fig. 5 secant undrained Young Modulus values are presented for the different binder/soil combinations investigated. These are calculated on the basis of the UCS test response, at the 50% of the compressive strength and on treated samples after 28 days of curing. As with strength, the higher stiffness is conferred by the MK geopolymer mix. In the CS-treated samples with 40% of silica concentration, a clear trend of stiffness increase with permeability is evident. For the other two binders, a plateau/slight decrease in stiffness is observed when reaching the higher values of base-soil hydraulic conductivity (i.e. between 10^{-5} and 10^{-4} m/s).

When comparing the stress-strain response of the same base soil permeated with CS and resin, it is remarkable to note that the resin confers higher strengths and a more ductile response than CS. Indeed, CS-treated samples always presented higher stiffness than the resin treated ones, but lower strengths (Figs. 2, 5 and 6). This behaviour reflects the evolution of these binders: while CS solidifies within few days, resin remains with a jelly consistency for longer periods, in humid environments. MK-treated samples exhibited a similar response to CS-treated ones, in terms of axial strain at stress peak (Fraccica et al. 2022b).

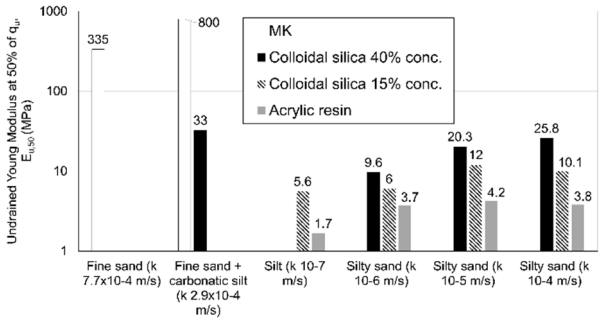

Figure 5. Secant Young Modulus at 50% of the unconfined compressive strength, for the different binders and soil combinations.

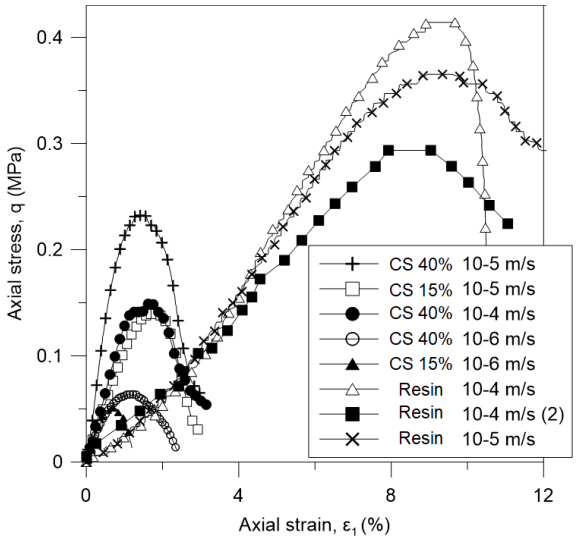

Figure 6. UCS tests on CS-treated samples (concentration of 40% and 15%) and on resin-treated samples.

3.3. Permeability

Fig. 7 shows the hydraulic conductivity values resulting from the treatment with MK and colloidal silica (with 40% concentration). No permeability tests were run on samples treated with acrylates. The results correspond always to specimens cured under "dry" conditions. The permeability of soil-geopolymer mixtures was measured in a triaxial cell under controlled gradient as described by Spagnoli et al. (2022b). Whereas for Fraccica et al. (2022a) the values of saturated water permeability calculated during the saturation stage of the TX tests.

From Fig. 7 it is possible to observe that the colloidal silica treatment reduced soil permeability by an order of magnitude more than the MK, even if they were dosed to attain the same target void filling ratio (see Fraccica et al. 2022). That the target was correctly attained was verified using computed tomography image analysis to measure the "as-cured" void ratio (see Spagnoli et al. 2022b for more detail).

The various microstructural characteristics of the binders, as seen by microscopy, provide a likely explanation for this variation (SEM and FESEM). The microstructure of colloidal silica is only heterogenous at the nanoscale and has smaller pores than those found in the MK (Porcino et al. 2011; Wong et al. 2018), but the metakaolin geopolymer exhibits micro-scale heterogeneity (Kuenzel et al. 2012; Spagnoli et al. 2022b).

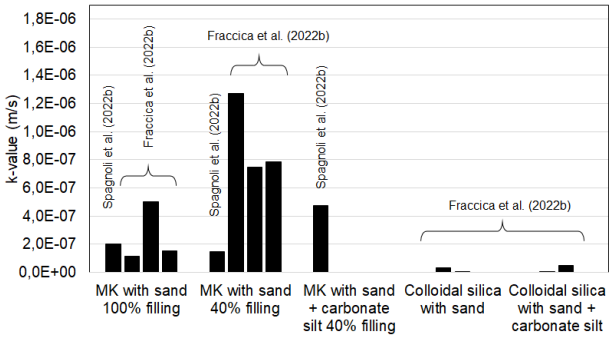

Figure 7. Hydraulic conductivity values on MK and colloidal silica treated soils (modified after Spagnoli et al. and 2022b and Fraccica et al. 2022b).

Therefore, some characteristics of the induced microstructure can be used to explain the observed differences between colloidal silica and MK treated soils. Both binders close up spaces between soil grains, gluing them together. The colloidal silica cement bridges, which have nanoscale porosity, have a much smoother texture (see Wong et al. 2018) than the MK geopolymer, which exhibits extensive retraction cracking at the microscale (Spagnoli et al. 2022b).

3.4. X-Ray tomography

X-ray CT scans were performed on untreated and treated soil samples, after 28 days of curing. The average X-ray energy was 130 keV and the voxel size was of 0.4x0.4x1.5mm^3. Results were provided in terms of grey value 3D-coloured maps (Fig. 8), given that grey values increase in correspondence with denser materials and chemical elements with larger atomic numbers. An increase of the grey values was observed in the treated samples, with comparison to the respective untreated ones (Fraccica et al. 2022a). X-ray scans allowed to check the homogeneity of the injection. Some anomalies were detected in the samples with permeability $k = 10^{-6}$ m/s, where the binders appeared sometimes to have found a preferential permeation path at soil/mould interfaces, during permeation. It was also observed that the compaction layers were sometimes offering preferential flow paths (Fig. 8).

In the treated samples with initial hydraulic conductivity $k = 10^{-4}$ m/s a more dispersed distribution of high-density clusters appeared, suggesting that the higher presence of macro-pores within this soil mixture affected the injection flow and the binder's arrangement in the matrix.

3.5. Injection performance

Grout permeation depends on numerous factors including injection pressure and flow rate, grout rheology, and its evolution over time (Raffle and Greenwood 1961) and the intrinsic permeability of the host soil (itself dependent on porosity, grain size distribution and other factors (Kim et al. 2009).

For several tests performed by Fraccica et al. (2022a;b), during the injection process, pressures and volumes were tracked by a pressure-volume controller (GDS) on water flowing into a water/binder interface, which allowed to transfer the pressure from one fluid to the other. Fig. 9 provides the injection trends observed for the different binders, in terms of injected binder volume normalised by the volume of the pre-treatment pores. The system allowed injection volumes higher than 100% of the volume of the pores as the fluids were allowed to overflow from the top of the sample. The three binders injected showed similar trends, justified by comparable values of viscosity. The higher the pre-treatment permeability, the larger the volume that was let to pass during the injection, which lasted 45 minutes in all cases. Above the permeability $k = 10^{-6}$ m/s the three binders flowed easily through soils with a flow volume greater than the volume of the voids while below that value, the acrylic resin seemed to reach the best performance. Comparison of these results with the X-ray images made it possible to assess that, although there were preferential flow paths or some binder's cluster formations, the permeation of the binders was fairly homogenous along the height of the soil samples. This quality check was also useful in choosing the samples to be further tested (mechanical and hydraulic investigations), cutting some soil portions that possibly were not permeated or discarding the worst samples.

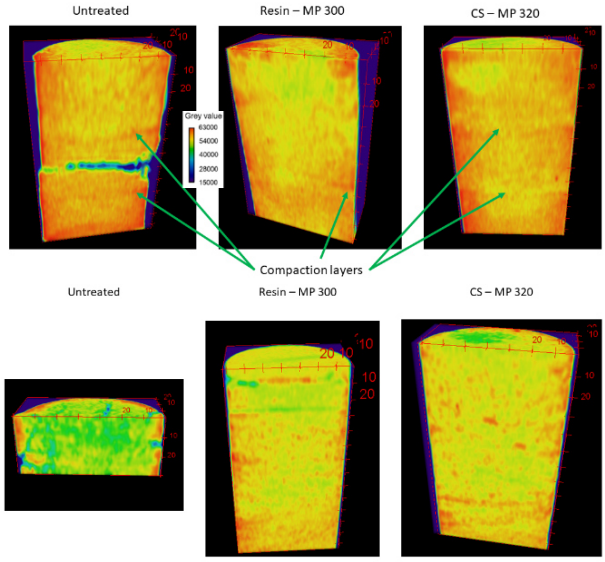

Figure 8. Grey values 3D coloured maps from X-ray CT scans on silty sand with untreated k = 10-6 m/s: a) untreated conditions b) after treatment with resin, c) after treatment with CS. 3D maps of silty sand with untreated k = 10-4 m/s: d) untreated conditions, e) after treatment with resin, f) after treatment with CS.

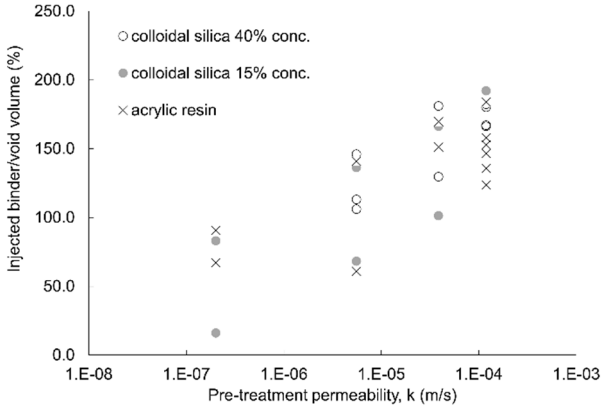

Figure 9. Injection performance in terms of injected volume of binder normalized by the pre-treatment volume of pores.

4. Conclusions

There is an increased interest in the study of novel binders for ground improvement purposes that can help reduce the reliance on OPC of these technologies. The test campaign that has been summarized in this paper illustrates that it is useful to test different products simultaneously to better perceive the singular aspects of each material and that it is also useful to supplement standard geotechnical test with microscale investigations, as the latter can help understand the trends observed at specimen scale.

References

Axelsson, M., 2006. "Mechanical tests on a new non-cementitious grout, silica sol: a laboratory study of the material characteristics." Tunn. Undergr. Space Technol. 21, 554–560.

Colombo, P., F. Colleselli, 1996. *Elementi di Geotecnica*. Zanichelli, Bologna.

Croce, P., A. Flora, and G. Modoni, 2015. *Jet Grouting*. CRC Press, Boca Raton, Florida.

Han, J. 2015. *Principles and Practices of Ground Improvement*. Wiley, Hoboken, New Jersey.

Fraccica, A, 2019. *Experimental Study and Numerical Modelling of Soil-Roots Hydro-Mechanical Interactions*. PhD Thesis. Université Montpellier; Universitat Politécnica de Catalunya.

Fraccica, A., G. Spagnoli, E. Romero, M. Arroyo, and R. Gomez, 2022a. "Permeation Grouting of Silt-Sand Mixtures." Transp Geotech 35: 100800. https://doi.org/10.1016/j.trgeo.2022.100800

Fraccica, A., G. Spagnoli, E. Romero, M. Arroyo, and R. Gomez, 2022b. "Exploring the Mechanical Response of Low-Carbon Soil Improvement Mixtures." Can Geotech J, 59, No. 5, https://doi.org/10.1139/cgj-2021-0087 (ahead of print).

Fraccica, A., G. Spagnoli, E. Romero, and M. Arroyo, 2022c. "Impact of Colloidal Silica Treatment on an Earthfill Dam." In *Geo-Congress 2022*, edited by A. Lemnitzer, and A.W. Stuedlein, 167-178. Reston, VA: ASCE. https://doi.org/10.1061/9780784484012.017

Fraccica, A., G. Spagnoli, E. Romero, and M. Arroyo, 2023. "Evaluating the Potentiality of X-Ray Tomography on the Quality Assessment of Grouted Soils." In *IACMAG 2022: Challenges and Innovations in Geomechanics*, edited by M. Barla, A. Di Donna, D. Sterpi, and A. Insana, 3-10. Cham: Springer. https://doi.org/10.1007/978-3-031-12851-6_1

International Energy Agency, 2018. *Technology Roadmap: Low-Carbon Transition in the Cement Industry*, IEA.

Kendall, A., A.J. Raymond, J. Tipton, and J.T. DeJong, 2017. "Review of Life-Cycle-Based Environmental Assessments of Geotechnical Systems." Proc Inst Civ Eng- Eng Su, 171, No. 2: 57-67.

Kim, J. S., I.M. Lee, J.H. Jang, and H. Choi, 2009. "Groutability of cement-based grout with consideration of viscosity and filtration phenomenon." Int. J. Numer. Anal. Methods Geomech., 33, No. 16: 1771-1797.

Kuenzel, C., L.J. Vandeperre, S. Donatello, A.R. Boccaccini, and C. Cheeseman, 2012. "Ambient Temperature Drying Shrinkage and Cracking in Metakaolin-Based Geopolymers." J Am Ceram Soc, 95 No. 10: 3270-3277.

Lehne, J. and F. Preston, 2018. *Making Concrete Change*. The Royal Institute of International Affairs, London.

Mohammed, M.A., N.Z.M. Yunus, M.A. D.Z.A. Hezmi, Hasbollah, and A.S.A. Rashid, (2021). Ground Improvement and its Role in Carbon Dioxide Reduction: a Review. Environ Sci Pollut Res, 1-21. https://doi.org/10.1007/s11356-021-12392-0

Moseley, M.P., and K. Kirsch, 2004. *Ground Improvement*. Spon Press, Oxon.

Nicholson, P.G. 2015. *Soil Improvement and Ground Modification Methods*. Elsevier, Oxford.

Persoff, P., J .Apps, G. Moridis, and J.M. Whang, 1999. "Effect of Dilution and Contaminants of Sand Grouted with Colloidal Silica." J Geotech Geoenvironmental Eng, 125 No. 6: 461-469.

Porcino, D., V. Marcianò and R. Granata, 2011. "Undrained Cyclic Response of a Silicate-Grouted Sand for Liquefaction Mitigation Purposes." Geomech Geoengin, 6 No. 3: 155–170. http://dx.doi.org/10.1080/17486025.2011.560287

Raffle, J.F., and D.A. Greenwood, 1961. The relationship between the rheological characteristics of grouts and their capacity to permeate soils. *Proc. 5th Int. Conf on Soil Mech. & Found. Engng.*, Vol. 2, 789-793.

Salvatore, E., G. Modoni, G. Spagnoli, M. Arciero, M.C. Mascolo, and M. Ochmański, 2022. "Conditioning Clayey Soils with a Dispersant Agent for Deep Soil Mixing Application: Laboratory Experiments and Artificial Neural Network Interpretation." Acta Geotech, 17: 5073–5087. https://doi.org/10.1007/s11440-022-01505-9

Shillaber, C.M., J.K. Mitchell, and J.E. Dove, 2016. "Energy and Carbon Assessment of Ground Improvement Works. I: Definitions and Background." J Geotech Geoenvironmental Eng, 142, No. 3: 04015083. https://doi.org/10.1061/(ASCE)GT.1943-5606.0001410

Spagnoli, G. 2021. "A Review of Soil Improvement with Non-Conventional Grouts." Int J Geotech Eng 15 no. 3: 273-287. https://doi.org/10.1080/19386362.2018.1484603

Spagnoli, G., W. Seidl, E. Romero, M. Arroyo, R. Gomez, and J. Lopez, 2021. "Unconfined Compressive Strength of Sand-Fines Mixtures Treated with Chemical Grouts." In *Geotechnical Aspects of Underground Construction in Soft Ground*, edited by M.Z.E.B. Elshafie, G.M.B. Viggiani, and R.J. Mair, 829-835. Boca Raton, FL: CRC Press. https://doi.org/10.1201/9780429321559-109

Spagnoli, G., G. Modoni, M. Arciero, and E. Salvatore 2022a. "Improving the hydrodynamic performance of jet grouting with chemical additives." Int J Geosynth Ground Eng, 8 no. 1. https://doi.org/10.1007/s40891-021-00345-z

Spagnoli, G., E. Romero, A. Fraccica, M. Arroyo, and R. Gomez, 2022b. "The Effect of Curing Conditions on the Hydromechanical Properties of a Metakaolin-Based Soilcrete." Geotechnique, 72, No. 5: 455–469. https://doi.org/10.1680/jgeot.20.P.259

Spagnoli, G., and G. Tintelnot, 2022c. "Mechanical Properties of a Sand Injected with a Colloidal Silica Binder with Different Dilution Grades." Int J Geosynth Ground Eng, 8 no. 47, https://doi.org/10.1007/s40891-022-00391-1

Wong C., M. Pedrotti, G. El Mountassir, and R.J. Lunn, 2018. "A Study on the Mechanical Interaction between Soil and Colloidal Silica Gel for Ground Improvement." Eng Geol 243: 84-100.